

GREEN SYNTHESIS OF COPPER NANOPARTICLES FROM *MYRTUS COMMUNIS* LEAVES EXTRACT: CHARACTERIZATION, ANTIOXIDANT AND CATALYTIC ACTIVITY

A. K. Al-Jubouri
Researcher

N. H. Al-Saadi
Prof.

M. A. Kadhim
Assist. Prof.

Department of Chemistry, College of Science, University of Kerbala, Kerbala-Iraq

Corresponding author email: narjis.h@uokerbala.edu.iq; mohammed.abid-alhur@uokerbala.edu.iq; ayat.k@uokerbala.edu.iq

ABSTRACT

A simple, cost-effective, and environmentally friendly method for making green nanoparticles has been developed. The current study examines the use of *M. communis* leaves extract in the biosynthesis of copper nanoparticles (CuNPs). The color change and UV-visible spectrophotometer, which showed a distinct peak at 481nm, confirmed the formation of these particles. Different techniques were used to characterize copper nanoparticles. The influential functional groups that can bio-reduce the copper ion Cu^{2+} were identified using Fourier Transform Infrared (FT-IR) spectroscopy. The crystal structure of copper nanoparticles was determined using X-ray diffraction (XRD), as evidenced by the peaks at 2θ values of 43.35, 50.50, and 74.21. In transmission electron microscopy (TEM), the particles have spherical morphology with an average diameter of 35–75 nm, while scanning electron microscopy (SEM) reveals the sphere-like shape of CuNPs. Copper-NPs synthesized in this study were tested as antioxidant and catalytic substances. CuNPs had superior radical scavenging activity when compared to an extract from *Myrtus communis* leaves. It is common to use 4-nitrophenol (4-NP) as a model reaction to evaluate synthesized nanomaterials' catalytic properties. borohydride (BH) was found to bind to the surface of CuNPs, indicating that it is an adsorbent. As the BH concentration increased, we observed a blue shift in the surface plasmon resonance (SPR) of CuNPs. These shifts increase in direct proportion to BH concentration, as does 4-NP to 4-amino phenol (4-AP) conversion. Accordingly, CuNPs have better catalytic activity than extract at higher BH concentrations .

Keywords: nanoparticles, *Myrtus communis*, Plant extracts, catalytic activity.

الجبوري وآخرون

مجلة العلوم الزراعية العراقية - 2022: 53(2): 471-486

التخليق الأخضر لجسيمات النحاس النانوية من مستخلص أوراق نبات الياس: التوصيف، ومضادات الأكسدة والنشاط التحفيزي

محمد عبد الحر كاظم

نرجس هادي السعدي

آيات كريم الجبوري

استاذ مساعد

استاذ

باحث

قسم الكيمياء ، كلية العلوم ، جامعة كربلاء

المستخلص

تم تطوير طريقة بسيطة وفعالة من حيث التكلفة وصديقة للبيئة لصنع الجزيئات النانوية الخضراء. تهدف الدراسة الحالية الى استعمال مستخلص أوراق نبات الياس في التخليق الحيوي لدقائق النحاس النانوية. أكد تغير اللون ومقياس الطيف الضوئي المرئي للأشعة فوق البنفسجية الذي أظهر قمة مميزة عند 481 نانومتر ، تكوين هذه الدقائق. استخدمت تقنيات مختلفة لتوصيف دقائق النحاس النانوية. تم تشخيص المجموعات الوظيفية المؤثرة التي يمكنها اختزال أيون النحاس Cu^{2+} باستعمال مطيافية الأشعة تحت الحمراء (FT-IR). حدد التركيب البلوري للجسيمات النانوية النحاسية باستعمال حيود الأشعة السينية (XRD) ، كما يتضح من القمم عند 2θ قيم 43.35 و 50.50 و 74.21. اما تقنية المجهر الإلكتروني النافذ (TEM) بينت ان الجسيمات تمتلك شكلاً كروياً يبلغ متوسط قطرها 35–75 نانومتر ، بينما كشف الفحص المجهر الإلكتروني الماسح (SEM) عن الشكل الشبيه بالكرة لدقائق النحاس النانوية. تم اختبار دقائق النحاس النانوية المحضرة في هذه الدراسة كمضادات أكسدة وامتلاكها النشاط التحفيزي. اظهرت النتائج ان دقائق النحاس النانوية لها نشاط لكسح الجذور الحرة عند مقارنتها بمستخلص من أوراق نبات الياس. من الشائع استعمال 4-نيتروفينول (4-NP) كتفاعل نموذجي لتقييم الخصائص التحفيزية للمواد النانوية المحضرة. اذ وجد أن بوروهيدريد (BH) يرتبط بسطح نحاس ، مما يشير إلى أنه مادة ماصة. مع زيادة تركيز BH ، لوحظ تحولاً أزرق في رنين البلازمون السطحي (SPR) لدقائق النانوية وتزداد تحولات SPR مباشرة مع زيادة تركيز BH ، كما هو الحال مع تحويل 4-NP إلى 4-amino phenol (4-AP) . وعليه تظهر النتائج أن دقائق النحاس النانوية لها نشاط تحفيزي أفضل من المستخلص عند التراكيز العالية من BH.

الكلمات المفتاحية: الجسيمات النانوية، نبات الياس، المستخلصات النباتية، النشاط التحفيزي

Received:14/12/2020, Accepted:22/3/2021

INTRODUCTION

Because of their size and shape, metallic nanoparticles can be used in a wide variety of fields. They've been used extensively in many fields, such as drug delivery, cancer treatment, wastewater treatment, DNA analysis, anti-bacterial agents, biosensors, solar power generation, and catalysis (21). Physical, chemical, and biological methods can all be used to make nanoparticles. Laser ablation, arc discharge, energy-high ball milling, and chemical vapor deposition are physical techniques. Hydrothermal, sonochemical, and microwave are chemical methods in addition to co-precipitation and sol-gel (3). Many limitations exist when using chemical or physical methods to synthesize copper nanoparticles, such as the high cost of reagents, production of toxic chemicals that are hazardous to health, and the time it takes to isolate the nanoparticles. As a result, it motivates scientists to devise new methods for synthesizing nanoparticles that use less expensive raw materials while also creating reaction conditions that are less hazardous and environmentally friendly. The use of bio-organisms in synthesis is in keeping with green chemistry ideals. The "green synthesis" of nanoparticles utilizes reagents that are non-toxic, environmentally friendly, and safe. Oxidation/reduction is the primary action during nanoparticle production in biosynthetic. Proteins, enzymes, and phytochemicals with antioxidant or reducing properties present in plant extracts reduce metal compounds into their respective nanoparticles (28). The diameter of a nanoparticle is less than one hundred nanometers (nm). Small size and high surface-to-volume ratio distinguish nanoparticles from bulk materials in terms of physicochemical properties (30). Copper (Cu) has numerous anti-inflammatories, anti-cancer, analgesic, and antimicrobial effects, making it a valuable medical element. The high surface-to-volume ratio of CuNPs has been demonstrated in recent years, which has led to various biological activities due to their high reactivity (14). Due to the abundance of biological entities, diversity, and environmentally acceptable production methods, the use of plant extracts to make CuNPs has gained popularity (13). Copper-

NPs synthesis has piqued researchers' interest because it is less expensive than obtaining silver or gold. Copper-NPs research has progressed significantly in the last decade due to its numerous applications in nanotechnology and nanomedicine, including catalysis, optics, electrical, and antifungal/antibacterial treatment (4). Plant crude extracts contain secondary metabolites like phenolic acid, flavonoids, alkaloids, and terpenoids. Ionic nanoparticle production in bulk metal nanoparticles is being reduced thanks to these compounds. The redox reaction that generates environmentally friendly Nanoparticles of various sizes involves both primary and secondary metabolic products (17). Several plant extracts, such as *Magnolia kobu*, *Terminalia arjuna*, *Aloe vera*, *Bifurcaria bifurcate*, and *Taber-naemontana*, have been used to synthesize copper-based nanoparticles (10). *Myrtus communis* plant has many traditional uses that have been validated by scientific research. Some of its clinical and pharmacological activities include anti-diarrheal, anti-ulcer, antidiabetic, antihypertensive, and antioxidant properties, as well as antimicrobial and inflammatory properties. It's non-toxic and biodegradable, as well as being environmentally friendly. *M. communis* is a therapeutic herb used in traditional medicine all over the world (8). By reducing copper ions in *M. communis* leaves extract, we examined the biosynthesis of copper nanoparticles. CuNPs were also tested for stability. Copper nanoparticle synthesis and particle size were studied about reaction conditions such as reaction temperature and $\text{CuSO}_4 \cdot 5\text{H}_2\text{O}$ concentration. The antioxidant and catalytic activity of the biosynthesized CuNPs was also evaluated.

MATERIALS AND METHODS

Plant Collection

Myrtus communis fresh leaves were obtained from the garden of the University of Kerbala, College of Science. The leaves were cleaned with distilled water and rinsed with deionized water. The clean leaves were dried and crushed into small slices before being stored in a dark and dry place for future use. The plant was identified by the Botanist Dr. Nibal Muteer at the University of Kerbala, College of Education of Pure Science.

Preparation of *Myrtus communis* Leaves

Extract: The crude extract of *M. communis* was made by weighing 10 grams of dried leaves and adding them to 100 mL of deionized water. The mixture was warmed up at 50 °C by a hot plate for 10 minutes then filtered by Whatman No. 1 filter paper. The filtrate was used for synthesizing CuNPs.

Qualitative Phytochemical Analysis

GC-Mas : Gas chromatography and mass spectroscopy (GC- Mass; Agilent) were used to analyze the chemical ingredients of *M. communis* leaves' extract. This analysis was done at the University of Kashan, Iran. The instrument used electron ionization with two columns, Helium, Nitrogen, and zero air, as a carrier gas. The oven temperature was 400 °C. To identify the organic compounds in the extracts, the chromatograms of GC-Mass that can detect organic compounds were used and compared with reference spectra.

Synthesis of Copper Nanoparticles

Copper-NPs synthesized by mixing 10 mL of *M. communis* leaves extract with 10 mL of 1 mM CuSO₄·5H₂O aqueous solution (the pH of the extract was adjusted to pH 10 by adding 0.1 mM NaOH). The mixture was stirred continuously for 30 minutes at room temperature. The solution's color changed rapidly, indicating that the reduction happened quickly. Overnight, the mixture was left at room temperature. To obtain copper nanoparticles, the mixture was centrifuged at 8000 rpm for 15 minutes. The nanoparticles were purified and washed with deionized water and centrifuged three times before being used in the experiment. Using an air oven, the CuNPs pellets were dried and stored for future use (26).

Effect of Heating Time and Volume of Plant Extract on CuNPs Synthesis:

To measure the influence of heating time on the preparation of the aqueous extract of *M. communis* leaves. A 10 gm of leaves pieces were heated up to 50 °C with 100 mL of deionized water for (5, 10, and 15 min) respectively. The color change in the solution from yellow to brown was followed using UV-visible spectroscopy (UV-1800/ Kyoto, Japan) at different periods and choosing the best peak indicating the complete reducing of Cu ions. To measure the effect of extract volume, various volumes of aqueous

extract (3, 5, and 10 mL) respectively was added into 10 mL of (1mM) CuSO₄·5H₂O; the synthesized CuNPs were observed as a function of time of reaction using UV-visible spectroscopy at periods and follow the exchange of color with the time.

Effect of pH on Synthesis of CuNPs

Next, to know the effect of the pH on the synthesis process for CuNPs. To do so, six different pH values were used (5, 6, 7, 8,9, and 10) to evaluate the synthesis of CuNPs. Constant volume and concentration of CuSO₄·5H₂O (10 mL, 1mM) and temperature (50°C) were used in this experiment. Finally, the effect of pH values was analyzed using UV-visible spectroscopy.

Effect of CuSO₄·5H₂O Concentration on Synthesis of CuNPs

Many scientists mention that the concentration of precursors is also considered a significant parameter when nanoparticles are synthesized. In this experiment, the concentration of CuSO₄·5H₂O was optimized by varying the concentration of CuSO₄·5H₂O (1mM, 2mM, and 3mM) with the constant other factors, the volume of extract (10 mL), pH of the medium (10), and temperature (50°C). UV-visible spectroscopy was used to examine the influence of CuSO₄·5H₂O concentration.

Characterization of Copper Nanoparticles

Ultraviolet-Visible Spectroscopy: A change in color and UV-visible absorption spectra are used as indicators for synthesis to confirm the synthesis of CuNPs. Various time points were used to measure the solution mixture's absorbance, and the maximum absorption was determined using scanning at the 300-700 nm range.

Fourier Transform-Infrared (FT-IR) Spectroscopy

FT-IR analysis was done for both extract and synthesized CuNPs. FT-IR spectroscopy is commonly used to examine interactions between NPs and capping agents. Using this method, the interactions of the functional group and the metal NPs can be checked when two or more functional groups are present in the capping agent. The pellets of CuNPs were measured with the KBr disk in the wavenumber ranging from 400 to 4000 cm⁻¹ using Shimadzu (8400S)/Japan FT-IR spectrophotometer.

X-ray Diffraction Analysis

One of the best non-destructive techniques for characterizing crystalline materials has been X-ray diffraction (XRD). This approach is used to provide information on structures, phases, desired crystal orientation (texture), and other structural parameters, such as average crystal size, crystallinity, strain, and crystal defects. The synthesized copper nanoparticles were studied using (XRD) (Philips Xpert /Holland XRD) with Cu-K α radiation ($k=1.50456$) in the range of (10° to 80°). Different phases present in the synthesized samples were determined by X'pert high score software with search and match facility. The crystal size of the prepared samples was calculated using the Scherer equation as follows:

$$(1) \quad D = 0.9 \lambda / \beta \cos \theta$$

Where D is the average of crystal size, λ is the wavelength of X-ray, β is the half maximum of the full width, and θ is Bragg's angle in radians. Cu-K α radiation ($k=1.50456$) was used in the range of 10° to 80° .

Transmission Electron Microscopy (TEM)

The Transmission electron microscopy (TEM) made tremendous changes in the NPs' images that can provide the surface shape and size distribution (EM10C/Germany)

Scanning Electron Microscopy (SEM)

Particle size, surface roughness, and intermetallic distribution can all be determined using SEM. It also provides information on the porosity and homogeneity of the materials. Nanomaterial surface morphology is frequently studied using scanning electron microscopy (SEM). SEM (Tescan Mira3 SEM/French) is commonly used to examine conductive samples

Antioxidant Assay

The synthesized CuNPs from *M. communis* leaves extract was evaluated for their antioxidant activity using three methods. Ascorbic acid was used as a reference.

1,1- Diphenyl-2-picrylhydrazyl (DPPH) Radical Scavenging Assay

The ability of CuNPs for scavenging DPPH radicals was determined by Devi *et al* (5). A serial dilution of each CuNPs and *M. communis* extract was prepared (100, 50, 25, 20, 10, and 5 $\mu\text{g/mL}$). An equal volume of DPPH (0.135 mM in ethanol) and CuNPs

solution or *M. communis* extract (1mL) was mixed and left in the dark place at room temperature for 30 minutes. Control was prepared as above without adding an extract or CuNPs. Ascorbic acid was used as a positive control. The absorbance of the samples and that of control were estimated at 517 nm. The ability of *M. communis* extract and CuNPs to scavenge the DPPH radical was calculated as a percentage of inhibition.

$$\text{Inhibition\%} = [(A \text{ control} - A \text{ sample}) / A \text{ control}] \times 100 \quad (2)$$

where A is the absorbance

Total antioxidant assay

A method described by Al-musawi and Al-Saadi (1). was used to determine the combined antioxidant activity of CuNPs and *M.communis*. A 0.3 mL of each diluted extract and CuNPs prepared as described in the DPPH assay was mixed with 3 mL of the reagent solution (0.6 M sulfuric acid, 28 mM sodium phosphate, 4 mM ammonium molybdate). For 90 minutes, the tubes were covered and incubated at 95°C in a water bath. To determine the absorbance at 695 nm, the tubes were cooled to room temperature and then read with an ohmmeter. The control was made the same way as the experimental one, accepting CuNPs or extract. The amount of ascorbic acid equivalents used to measure antioxidant activity was used. The following equation used to measure the antioxidant activity:

$$\text{Total antioxidant \%} = [(A \text{ control} - A \text{ sample}) / A \text{ control}] \times 100 \quad (3)$$

Reducing power

The method described by Flaih and Al-Saadi was used (9) to figure out the reducing power. Copper-NPs and *M. communis* extract (1mL) at various concentrations (100, 50, 25, 20, 10, and 5 g/mL, respectively), were mixed with 1 mL of sodium phosphate buffer (pH 6.6) and 1 mL of 1% potassium ferricyanide. For 20 minutes, the mixture was incubated at 50°C . After that, tri-chloroacetic acid (TCA) solution (10%) was added to stop the reaction. The mixture was centrifuged at 7500 xg for 20 minutes. The supernatant (1.5 mL) solution was mixed with the 1.5 mL distilled water and 0.1 mL of ferric chloride solution (0.1%, w/v) and then left for 10 minutes. At a wavelength of 700 nm, the absorbance was determined. As

the absorbance of the reaction mixture grew, it became clear that the extract's and CuNPs' reducing power had increased as well.

Catalytic Activity

Metal nanoparticles were created by converting nitro compounds like 4-nitrophenol to amino compounds using sodium borohydride (12). A 4-nitrophenol solution (1.9 mL, 0.2 mM) was added to a 3mL cuvette containing freshly synthesized sodium borohydride (1mL, 0.2 M) solution. The absorbance was measured in a UV-vis spectrophotometer by comparing it to wavelengths in the cuvette. We added a 0.1 mL of CuNPs or *M. communis* extract with different concentrations of (100, 50, 25, 20, 10, and 5 µg/mL) to the cuvette that was shaken

vigorously for mixing before being placed in a UV-Vis spectrophotometer and scanned from 200 to 800 nm.

RESULTS AND DISCUSSION

Qualitative Phytochemical Analysis

GC-MS analysis: GC mass analysis of aqueous leaves extracts of *M. communis* detected the chemical compounds as a percentage of the area, representing the major compound. The chromatogram of the study showed eight peaks of most constituents (Figure 1). Most of these included (S)-2-methyl -1-dodecanol, Heptadecanoic acid, heptadecyl, Thiosulfuric acid (H₂S₂O₃), tri-fluoroacetic acid, n-tridecyl, carbonic acid, decyl dodecyl ester, octadecanoic acid, 9-hexadecenoic acid, and methyl ester (Table 1).

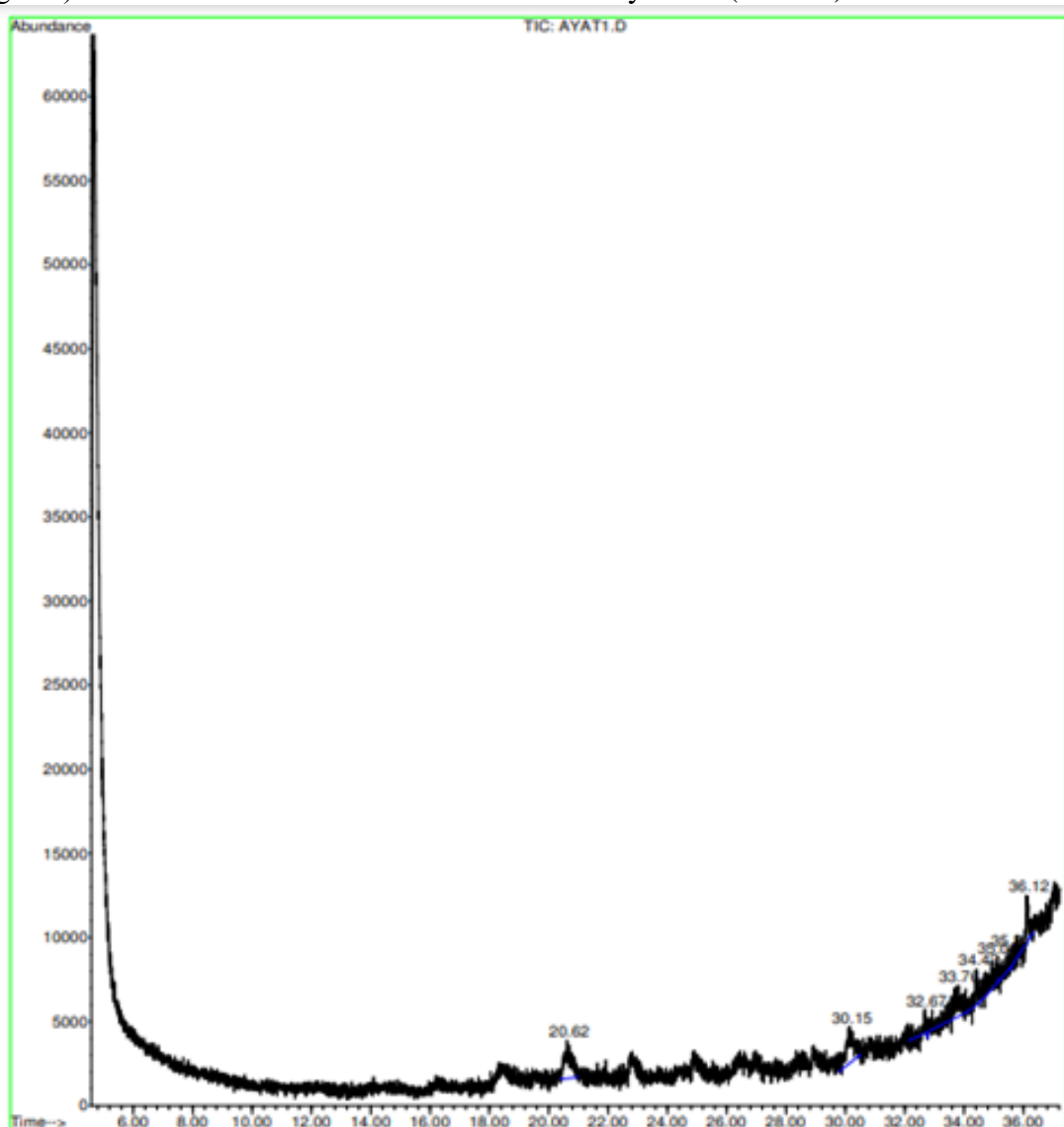


Figure 1. GC-MS of *M. communis* leaves extract

Table 1. GC-mass analysis of *M. communis* leaves extract

Peak	Retention Time	Area %	Name
1	20.62	18.38	(S)-2-methyl -1-dodecanol Hexyl octyl ether (RS)- n-Dodecyl trifluoromethyl carbinol
2	30.15	20.36	9-Hexadecenoic acid, methyl ester, (Z)- 1-Hexacosanol
3	32.67	2.73	Pentadecafluorooctanoic acid, octadecyl ester 1-Hentetracontanol Hexatriacontyl pentafluoropropionate
4	33.76	20.51	N-(2-Phenylethyl) undeca-(2Z,4E) Heptadecanoic acid, heptadecyl 14-.BETA.-H-PREGNA
5	34.42	7.36	9-Octadecenoic acid (Z) Heptadecanoic acid, heptadecyl
6	35.06	12.99	Thiosulfuric acid (H ₂ S ₂ O ₃) cis-Vaccenic acid 9-Octadecenoic acid
7	35.51	4.37	Iron, tricarbonyl Phenol, 4-bromo-2-(1,2-dimethyl Trifluoroacetic acid,n-tridecyl
8	36.12	13.30	Heptadecanoic acid, heptadecyl 9,10- Anthracenediol Carbonic acid, decyl dodecyl ester

Synthesis of Copper Nanoparticles

Green synthesis of CuNPs was achieved in an aqueous solution using *M. communis* extract as a reducing agent. When the extract was mixed with copper sulfate solution, the color of the aqueous solution changed immediately within 10 minutes, which turned dark brown within 24 hours indicated the formation of copper nanoparticles (Figure 2).

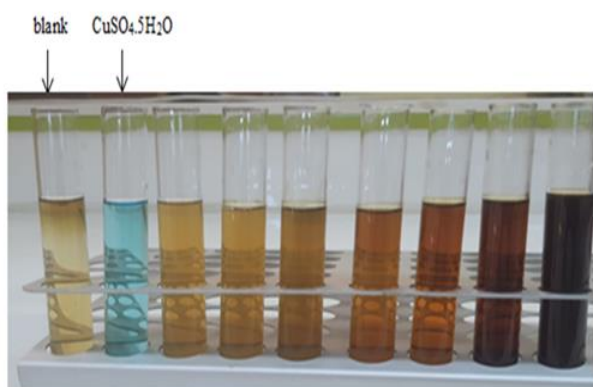


Figure 2. Biosynthesis of copper nanoparticles (CuNPs) and the color change with time

UV-Visible Spectroscopy Analysis

UV-visible spectroscopy confirmed the presence of CuNPs, and the peak at 481 nm was attributable to the presence of CuNPs (Figure 3a). To evaluate the optimal conditions for synthesis CuNPs, different effective

parameters were studied, the temperature at (5 min, 10 min, 15 min) and filtrate volume of extract (3 mL, 5 mL, 10 mL), different concentrations of copper sulfate (1mM, 2mM, 3mM), and effect of pH (5, 6, 7, 8, 9, 10). The optimal formation of CuNPs was obtained using 10 mL of the leaves extract (Figure. 3b), a boiling time of 10 minutes (Figure. 3c), the concentration of copper sulfate solution (1mM) (Figure. 3d), and pH 10 of leaves extract (Figure. 3e).

Fourier Transforms Infrared Spectroscopy (FT-IR)

The leaves extracted (Figure 4a) and manufactured CuNPs (Figure 4b) were subjected to FT-IR spectroscopy to identify the functional groups. Interestingly, the FT-IR spectrum of the leaves extract indicates intense bands at 3335.03 cm⁻¹ (O–H stretching vibrations), 2937.68 cm⁻¹ (C–H) and CH₂ vibration of aliphatic hydrocarbons), 1726.35 cm⁻¹ (C=O stretching vibration), 1616.40 cm⁻¹ (C=C stretching vibrations), 1452.45 cm⁻¹ (O–H bending vibrations), 1367.58 cm⁻¹ (C–O stretching of the ester group), 1240.27 cm⁻¹ (C–O asymmetric stretching in cyclic polyphenolic compounds) and 1039.67 cm⁻¹ (O–H deformation). When looking at synthesized CuNPs, the FT-IR spectrum shows

that the O-H groups are responsible for the broad peak at 3429.55 cm^{-1} ; however, signals in 2922.25 cm^{-1} are related to C-H asymmetric stretching aromatic rings (asymmetric stretching of C=O) as well as to stretching C=C and C-OH bending. *M. communis* extract interacts with Cu ions during bioreduction, as seen by the FT-IR spectra of CuNPs. *M. communis* extract peak locations and

absorption intensities were compared to those produced from CuNPs, and results showed that some band positions and absorption intensities from the plant extract peak were replicated in the CuNPs FT-IR spectrum. As a result of these findings, it can be concluded that the produced CuNPs are non-oxidative, pure, and coated with components of the *M. communis* extract

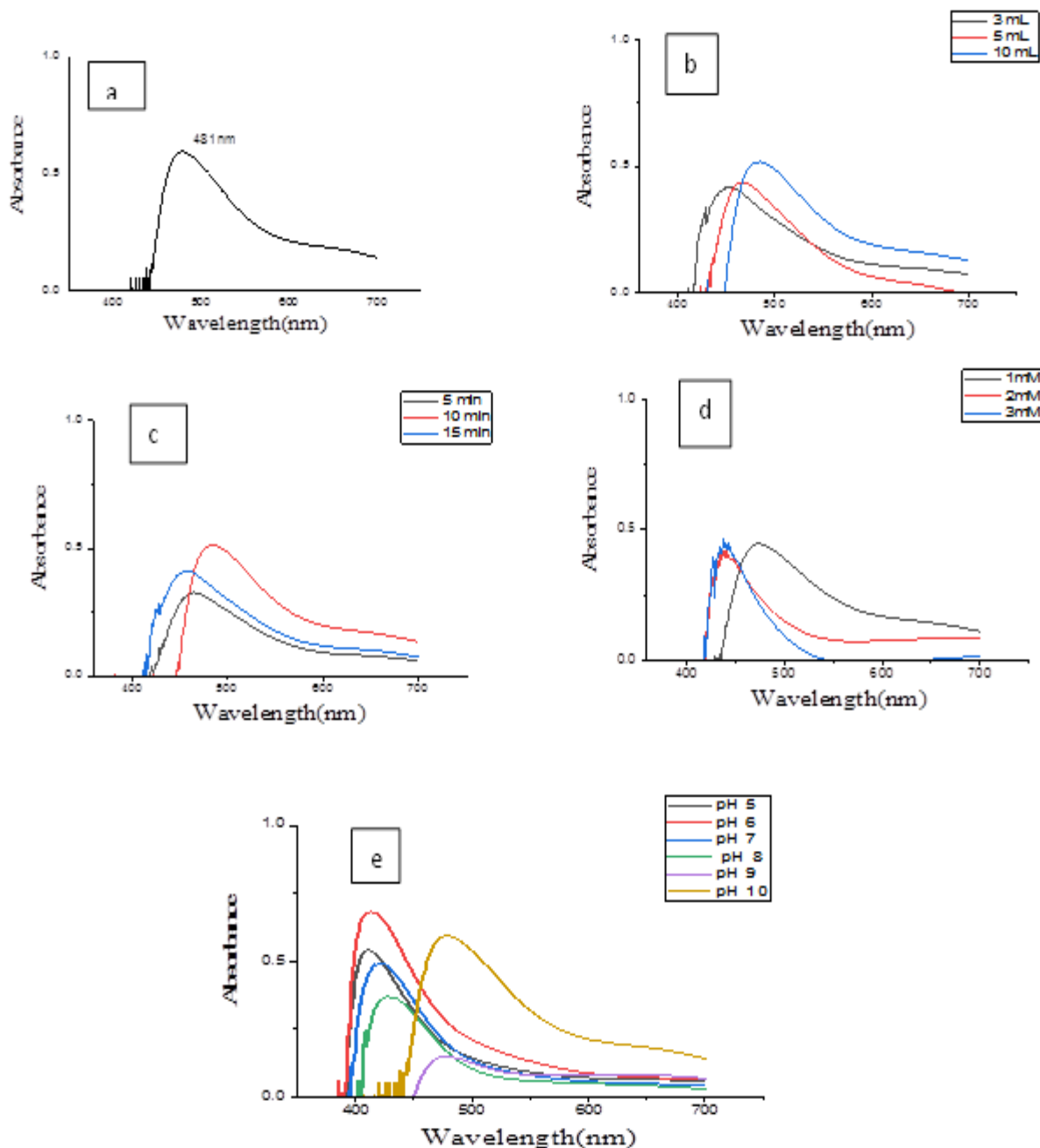


Figure 3. UV-visible spectra (a) for CuNPs (b) at different volumes of extract (c) at a different boiling time (d) at different $\text{CuSO}_4 \cdot 5\text{H}_2\text{O}$ concentrations (e) at different pH

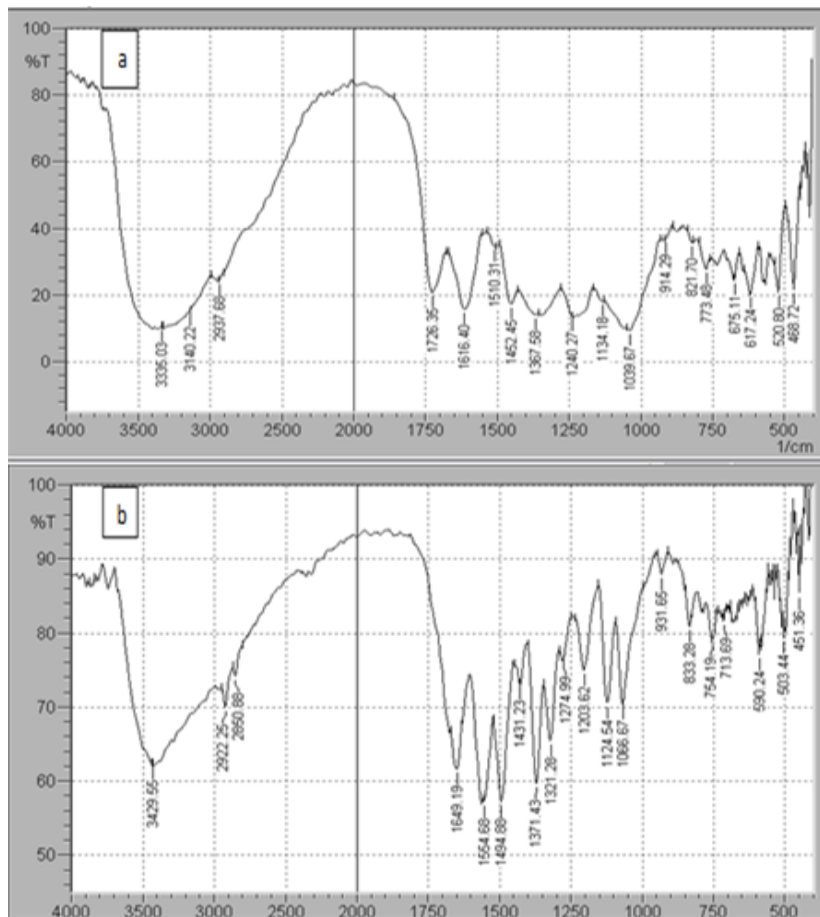


Figure 4. (a) (FT-IR spectrum of *M. communis* leaves extract) and (b) (FT-IR spectrum of CuNPs)

X-ray Diffraction (XRD)

Metallic Nano-powders can be identified by using XRD analysis. Scan angles ranged from 20 to 80 degrees for XRD patterns. The crystallinity of CuNPs was established by the diffraction pattern's peak positions (XRD). Copper-NPs have extremely strong diffraction lines, with three separate peaks seen at 2θ values of 43.43, 50.58, and 74.23°, respectively, and the values (111), (200), and (220) are Miller indices (Figure 5).

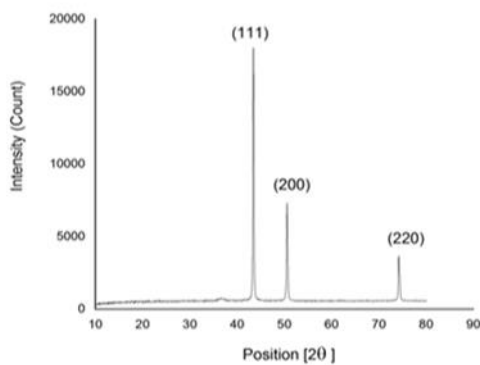


Figure 5. X-ray diffraction patterns for the synthesized CuNPs
Transmission Electron Microscopy (TEM)

The shape and size distribution of CuNPs were characterized by transmission electron microscopy analysis, (Figure 6a) showing CuNPs with spherical shapes. (Figure 6b) illustrates the TEM for the prepared CuNPs and the cumulating distribution of particle diameters. It seems that the particles of one mode of narrow and homogeneous distribution are limited from 35 to 70 nm diameter and of the average particle diameter of 55nm.

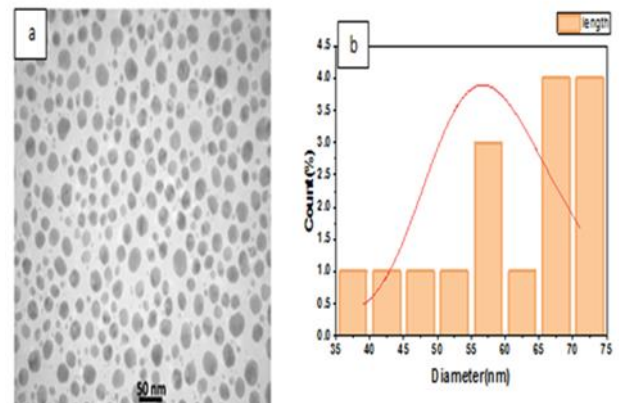


Figure 6. TEM images of biosynthesized CuNPs. (a) TEM image shows CuNPs with spherical and semispherical forms, (b) Distribution of CuNPs

Scanning Electron Microscope (SEM)

The morphological characteristics of the bio-synthesized copper nanoparticles were investigated by Scanning Electron Microscopy (SEM) analysis. SEM images showed that the

copper nanoparticles are predominately spherical, have a smooth surface, and are well dispersed with a close compact arrangement (Figure 7).

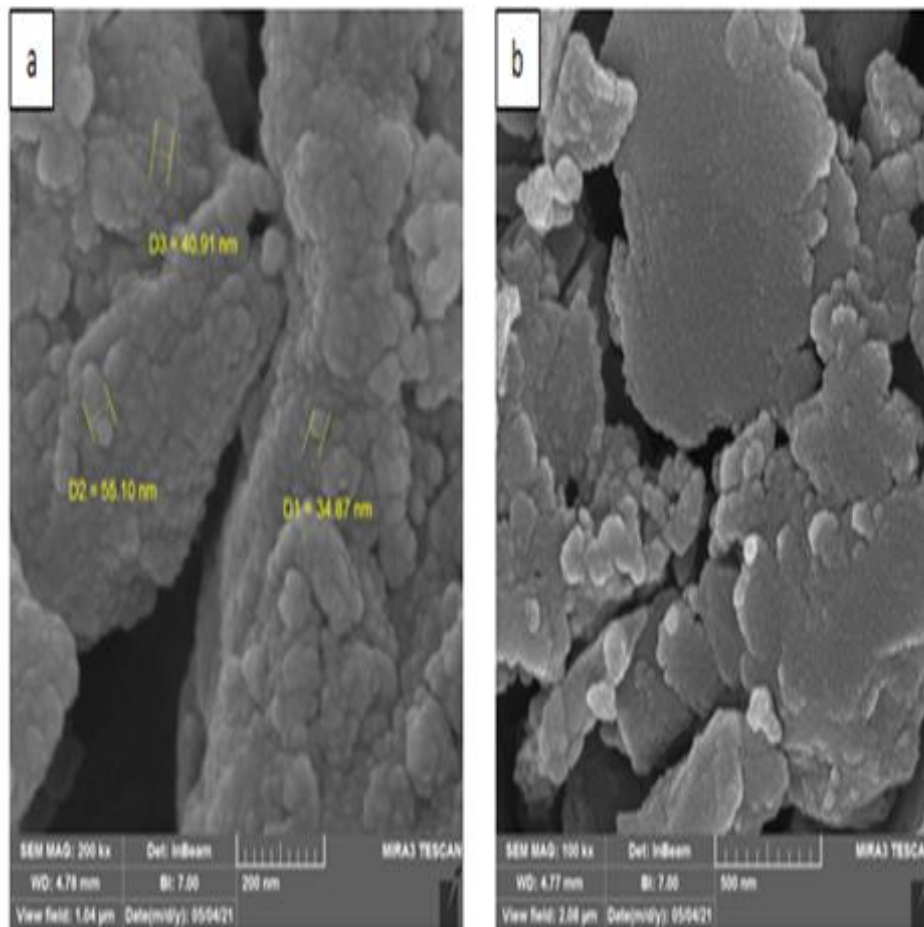


Figure 7. SEM image of biosynthesized copper nanoparticles (a) The particle size at different average diameters D1, D2, and D3. (b) SEM shows the spherical shape of particles

Antioxidant Activity of Copper Nanoparticles

In this study, three different assays were used to evaluate the antioxidant of the copper nanoparticles, DPPH, total antioxidant, and reducing power. DPPH scavenging capacity assay is the best choice among the three methods used because characterized by fast, stability, and simplicity. The results showed that CuNPs could scavenge free radicals compared with the *M. communis* leaves extract

and ascorbic acid used as a well-known standard antioxidant (Figure 8a). The total antioxidant capacity method determines the ability of a sample to donate electrons and neutralize free radicals. As shown in (Figure 8b), *M. communis* extract exhibited more potent antioxidant activity than CuNPs, whereas (Figure 8c) showed that CuNPs have higher antioxidant activity than *M. communis* extract. Their activity increased with the increase of concentrations.

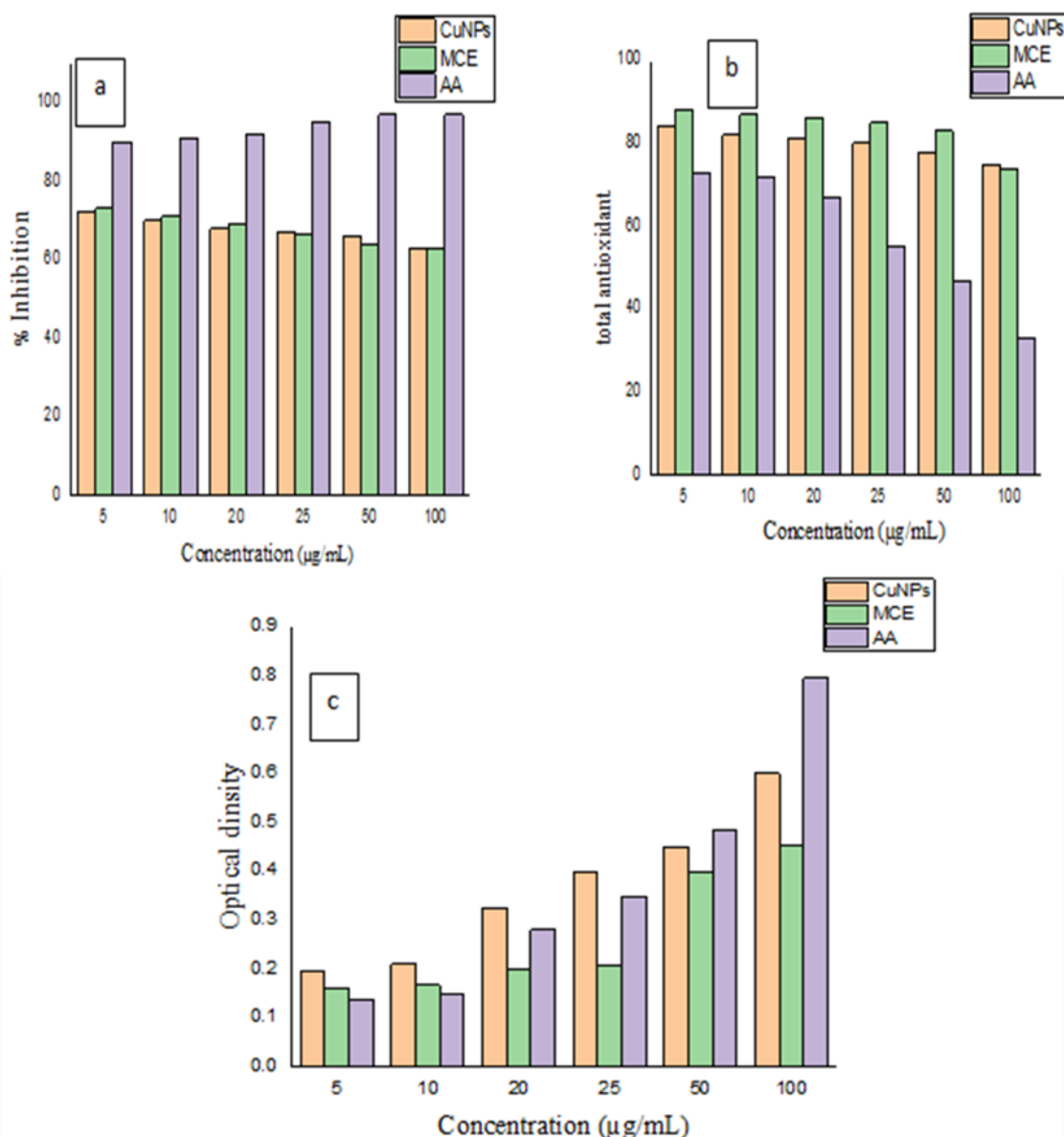


Figure 8. Antioxidant activity of the phyto-synthesized CuNPs and plant extract. (a) DPPH free radical scavenging assay (b) total antioxidant capacity assay (c) reducing power assay.

Ascorbic acid (A.A) as a reference (positive control)

Catalytic Activity of Copper Nanoparticles

In the presence of synthesized CuNPs, 4-nitrophenol (4-NP) reduction was studied using NaBH_4 . Pure 4-NP has a peak in absorption at 317 nm, and when NaBH_4 was added, a redshift occurred from 317 to 400 nm because of the production of 4-nitrophenolate (NP) ions. At high concentrations (100 µg/mL), the UV-visible absorption spectra showed that at 400 nm, the peak completely

disappeared after adding CuNPs. Furthermore, a new peak was observed at 298 nm within 15 minutes (Figure 9a), indicating the formation of 4-aminophenol. At low concentration (50, 25, 20, 10, 5 µg/mL), the peak at 298 nm after 15 minutes not formed. While the addition of extract at all concentrations, the peak at 400 nm remains, and no other peak formed (Figure 10).

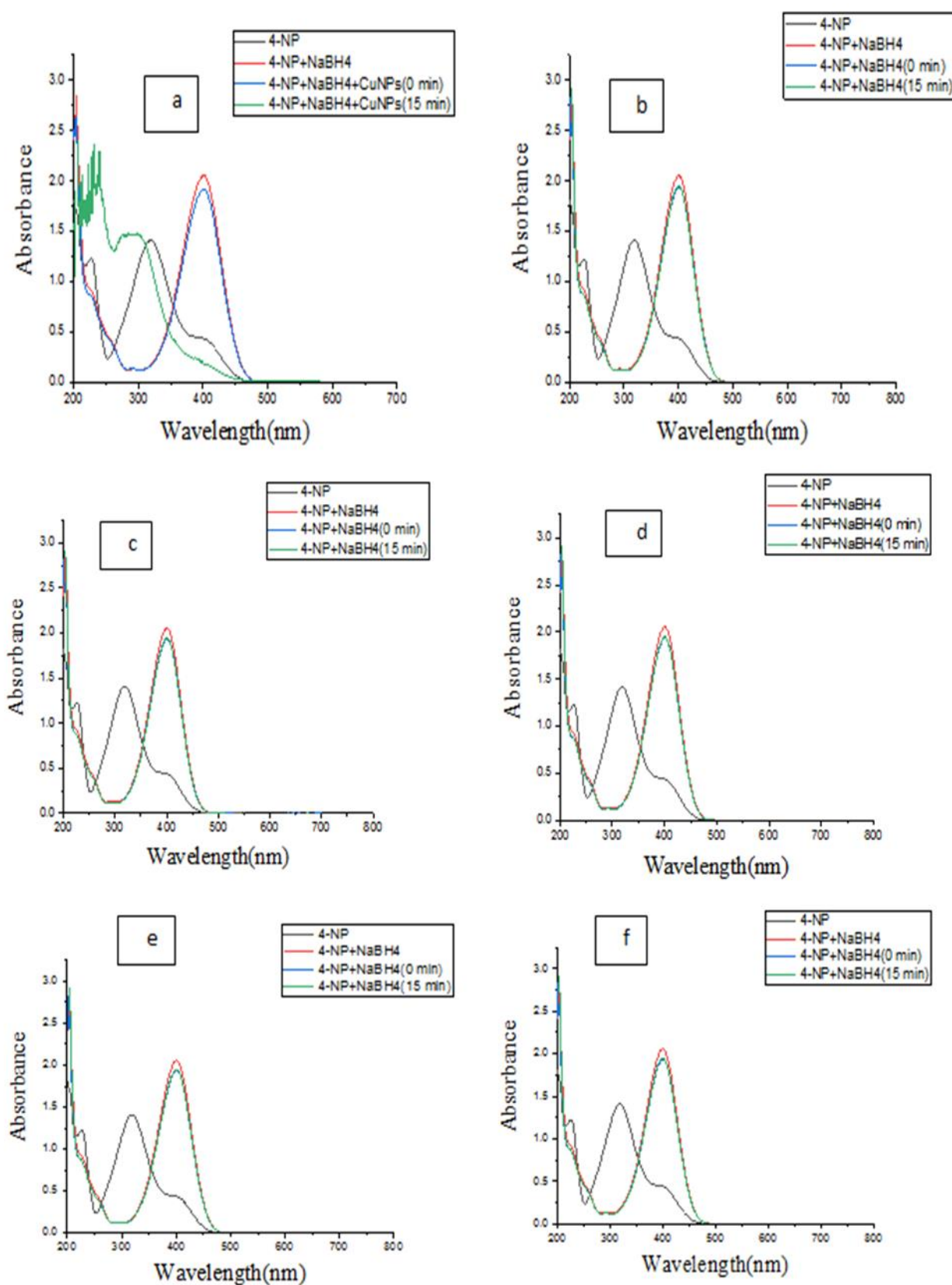


Figure 9. UV-visible spectra of the reduction of 4-NP by CuNPs at concentrations (a) 100 $\mu\text{g/mL}$ (b) 50 $\mu\text{g/mL}$ (c) 25 $\mu\text{g/mL}$ (d) 20 $\mu\text{g/mL}$ (e) 10 $\mu\text{g/mL}$ and (f) 5 $\mu\text{g/mL}$.

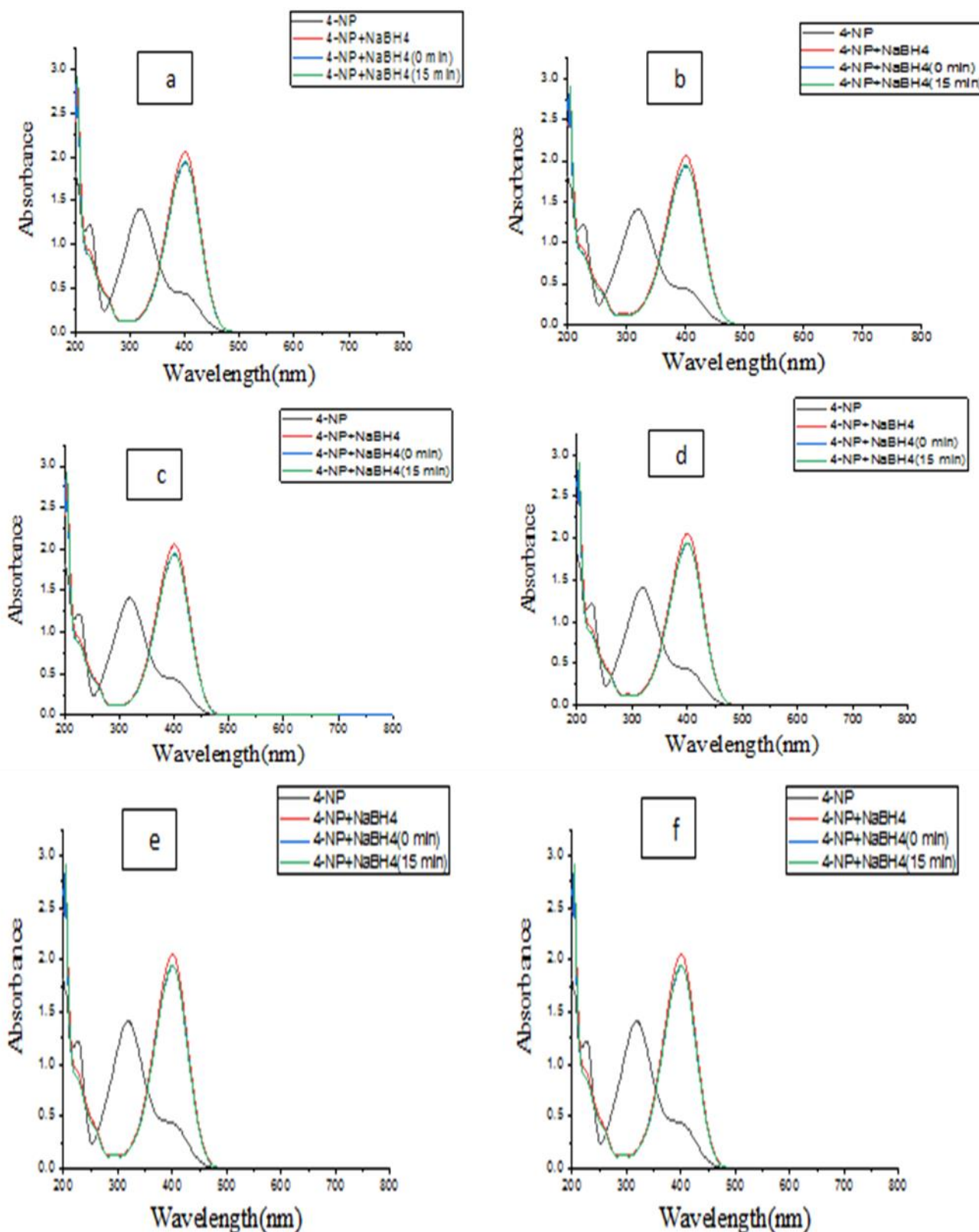


Figure 10. UV-visible spectrum of the reduction of 4-NP by *M. communis* at the concentrations (a) 100 µg/mL (b) 50 µg/mL (c) 25 µg/mL (d) 20 µg/mL (e) 10 µg/mL and (f) 5 µg/mL .

Environmentally friendly alternatives to chemical and physical methods for nanoparticle synthesis have been suggested, including biological methods utilizing

microorganisms, enzymes, and plants or extracts (18). The GC-MS analysis of *M. communis* leaves extract revealed the retention time (RT), area percentage, and component

names of phytochemical components (Table 1). Biological activity is present in the majority of these chemicals (19). The GC-MS analysis reveals the relative concentration of various components eluted as a fraction of retention time. GC-MS showed different peaks in the extract of *M. communis* leaves, and their heights indicate the relative concentration of the various compounds present. Octadecanoic acid hexadecanoic acid, and ethyl ester were found to be saturated fatty acids, and they may act as antioxidants, anti-androgenic, hemolytic, and alpha-reductase inhibitors (24). UV-visible absorption spectroscopy is one of the most valuable techniques for studying metal nanoparticle formation in aqueous solutions. The color change and UV-visible spectroscopy was used to track the reduction of aqueous metal ions, and subsequent formation of metal nanoparticles using *M. communis* leaves extract (26). The peak in UV-visible spectroscopy could be seen at 481 nm (Figure 3a). The highest absorbance value indicates that the copper ions have been completely reduced and that CuNPs have been synthesized quickly. To our surprise, we noticed an increase in synthesized CuNPs yield with an increased infiltrate volume (Figure 3b). This was due to high peak absorbance, which required a 10 mL extract and boiling for 10 minutes (Figure 3c). The least reaction ability was obtained by boiling the extract for five and fifteen minutes. A concentration of 1mM copper sulfate yields the best results (Figure 3d), while concentrations of 2mM and 3mM showed the lowest intensity of reaction (Figure 20) (29). The addition of leave extracts to $\text{CuSO}_4 \cdot 5\text{H}_2\text{O}$ had no effect on the formation of nanoparticles when pH was considered. CuNPs were obtained after the pH of the extract medium was changed to basic by adding 0.1 mM NaOH (Figure 3e). In the presence of CuNPs, the solution turned light brown (pH 5) and showed no absorption peak. It was found that the formation of CuNPs began at pH 10 and peaked at 481 nm, revealing their formation. However, as pH rises toward alkaline media, the rate of synthesis accelerates. CuNPs could be formed in alkaline conditions without agitating the mixture, and all of the copper ions added were converted to CuNPs in less

than 30 minutes (15). To better understand how functional groups interact with metal particles and biomolecules, FT-IR analysis is essential. FT-IR spectra were used to identify the biomolecules that cap and stabilize the copper nanoparticle in the current study. The difference in wavenumber between *M. communis* and CuNPs indicated the presence of a functional interaction group (7). In the FT-IR spectrum of copper nanoparticles, different organic molecules like terpenoids, alcohols, ketones, aldehydes, and carboxylic acid were found to be surrounding the copper nanoparticles (16). Analyzing the produced sample with XRD helped identify its crystal structure and phase composition (Figure 5). At $2\theta = 43.43^\circ$ (111), 50.58° (210), and 74.23° (220), the copper XRD peak represents the face-centered cubic structure and confirms the single phase of CuNPs obtained (2). Using transmission electron microscopy, the NPs' surface morphology and size distribution were analyzed (27). These results show that the CuNPs produced in this experiment have an almost-sphere-like particle morphology, with a diameter between 35 and 75 nm, as shown in Figure 6 (25). Figure 7 shows SEM images of synthesized CuNPs, which show slightly agglomerated, spherical NPs formed. The NPs' diameter is 55 nm on average. This study used three different assays to investigate the antioxidant activity of synthesized CuNPs and *M. communis* leaves extract because a single universal method cannot accurately assess antioxidant activity. Furthermore, DPPH \cdot (2,2-diphenyl-1-picrylhydrazyl) is regarded as a stable free radical due to the delocalization of the spare electron on the entire molecule. As a result, unlike most other free radicals, DPPH \cdot does not dimerize. Purple coloration is determined by the presence of delocalization on the DPPH \cdot molecule. The reduced (molecular) form (DPPH) is generated when DPPH \cdot reacts with a hydrogen donor, and the violet color is lost as a result (DPPH is reduced). This means that the decrease in absorbance is proportional to the antioxidant concentration (23), (11). Flavonoids, phenols, and other reducible agents in plants provide antioxidant power. Compounds with antioxidant activity can scavenge free radicals, donate hydrogen atoms or electrons, or chelate

metal cations (31). Additionally, the catalytic activity of the synthesized CuNPs was investigated in the reduction of 4-nitrophenol in an aqueous medium at room temperature in the presence of a solution of sodium borohydride in aqueous form; CuNPs can catalyze the reaction to overcome the kinetic barrier by transferring electrons from the donor borohydride ions to the 4-NP acceptor. A 4-AP is a critical intermediate in the production of analgesics and antipyretics that is commercially important. A 4-NP, a paracetamol synthesis intermediate, is one of the most refractory pollutants found in industrial wastewaters (20). At 317 nm, the absorption spectra of pure 4-NP show a distinct peak. (Figure 9). Adding NaBH₄ increased the 4-NP solution's yellow hue and caused a redshift from 317 to 400 nm because of the production of 4-nitrophenolate ions in the 4-NP solution, according to an initial experiment (22). Even after spending days at 400 nm with no catalyst, there was no decrease in 4-NP. CuNPs acted as a catalyst, and the 4-NP solution's yellow hue quickly faded until it vanished completely at a wavelength of 400 nm. A new peak at 298 nm was observed after only 15 minutes of adding 100 µg/mL of CuNPs. (Figure 9a). When compared to *M. communis*, CuNPs show superior 4-NP reduction catalytic activity. Reducing 4-NP may involve one of the following mechanisms: (Figure 11) The solution contains 4-NP ions as well as sodium borohydride. The protons of the borohydride ion bind to the copper nanoparticle surfaces and form BO₂⁻. 4-Nitrophenolate ions are also attracted to the surfaces of CuNPs. By adsorbing both protons and 4-nitrophenolate ions, CuNPs bypass the reaction's kinetic barrier, transforming the 4-nitrophenolate ion into the 4-aminophenolate ion. It is only after conversion that the 4-aminophenolate ion is desorption, that 4-aminophenol is formed (6).

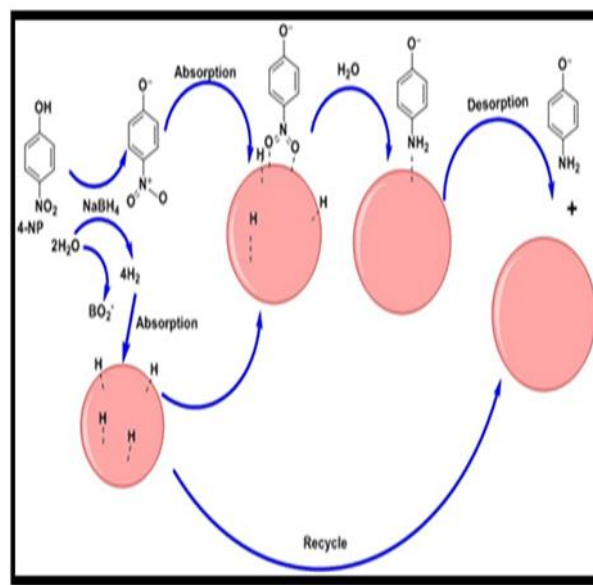


Figure 11. Mechanism of reduction of 4-nitrophenol (6).

Conclusions

The leaves extract of *M. communis* was used to synthesize CuNPs successfully. This method is easy, quick, and environmentally friendly to synthesize nanoparticles without using any hazardous chemicals. Copper nanoparticles were formed in the presence of phyto-constituents such as polyphenols and tannins, which played a role in reducing and capping agents. CuNPs were found to have superior antioxidant and catalytic activity when compared to the leaves extract of *M. communis* in this study.

REFERENCES

1. Al-musawi, Z. F., N. H., Al-saadi, and I. M. Ali, 2022. Antibacterial and Antioxidant Activities of Silver Nanoparticle Synthesized from *Dodonaea viscosa* L. Extract. 020029(5).
2. Betancourt-Galindo, R., P. Y., Reyes-Rodriguez, B. A., Puente-Urbina, C. A., Avila-Orta, O. S., Rodríguez-Fernández, G., Cadenas-Pliego, R. H., Lira-Saldivar, and L. A. García-Cerda, 2014. Synthesis of copper nanoparticles by thermal decomposition and their antimicrobial properties. *Journal of Nanomaterials*, 2014, 7–11. <https://doi.org/10.1155/2014/980545>
3. Caroling, G., M. N., Priyadharshini, E., Vinodhini, A. M., Ranjitham, and P. Shanthi, 2015. – Characterisation and Study of Antibacterial Effects. 5(2).
4. Chung, I., A. A., Rahuman, S., Marimuthu, A. V., Kirthi, K., Anbarasan, P., Padmini, and

- G. Rajakumar, 2017. Green synthesis of copper nanoparticles using eclipta prostrata leaves extract and their antioxidant and cytotoxic activities. *Experimental and Therapeutic Medicine*, 14(1), 18–24. <https://doi.org/10.3892/etm.2017.4466>
5. Devi, R. S., M., Jeevitha, S., Preetha, and S. Rajeshkumar, 2020. Free Radical Scavenging Activity of Copper Nanoparticles Synthesized from Dried Ginger. *Journal of Pharmaceutical Research International*, 32(19), 1–7. <https://doi.org/10.9734/jpri/2020/v32i1930703>
6. Din, M. I., F., Arshad, Z., Hussain, and M. Mukhtar, 2017. Green Adeptness in the Synthesis and Stabilization of Copper Nanoparticles: Catalytic, Antibacterial, Cytotoxicity, and Antioxidant Activities. *Nanoscale Research Letters*, 12. <https://doi.org/10.1186/s11671-017-2399-8>
7. Elisma, N., A., Labanni, Y., Emriadi, Rilda, M., Asrofi, and S. Arief, 2019. Green synthesis of copper nanoparticles using *Uncaria gambir roxb.* Leaf extract and its characterization. *Rasayan Journal of Chemistry*, 12(4), 1752–1756. <https://doi.org/10.31788/RJC.2019.1245347>
8. Eslami, S., M. A., Ebrahimzadeh, and P. Biparva, 2018. Green synthesis of safe zero valent iron nanoparticles by: *Myrtus communis* leaf extract as an effective agent for reducing excessive iron in iron-overloaded mice, a thalassemia model. *RSC Advances*, 8(46), 26144–26155. <https://doi.org/10.1039/c8ra04451a>
8. Flaih, L. S., and N. H. Al-Saadi, 2020. Green synthesis of silver nanoparticles from *Cassia obtusifolia* leaves extract: Characterization and antioxidant activity. *AIP Conference Proceedings*, 2290(December). <https://doi.org/10.1063/5.0027542>
9. Ghosh, M. K., S., Sahu, I., Gupta, and T. K. Ghorai, 2020. Green synthesis of copper nanoparticles from an extract of *Jatropha curcas* leaves: characterization, optical properties, CT-DNA binding and photocatalytic activity. *RSC Advances*, 10(37), 22027–22035. <https://doi.org/10.1039/d0ra03186k>
10. Gomaa, E. Z. 2017. Antimicrobial, antioxidant and antitumor activities of silver nanoparticles synthesized by *Allium cepa* extract: A green approach. *Journal of Genetic Engineering and Biotechnology*, 15(1), 49–57. <https://doi.org/10.1016/j.jgeb.2016.12.002>
11. Gondwal, M., and G. Joshi Nee Pant, 2018. Synthesis and Catalytic and Biological Activities of Silver and Copper Nanoparticles Using *Cassia occidentalis*. *International Journal of Biomaterials*, 2018. <https://doi.org/10.1155/2018/6735426>
12. Hassanien, R., D. Z., Husein, and M. F. Al-Hakkani, 2018. Biosynthesis of copper nanoparticles using aqueous *Tilia* extract: antimicrobial and anticancer activities. *Heliyon*, 4(12), e01077. <https://doi.org/10.1016/j.heliyon.2018.e01077>
13. Khatami, M., K., Ebrahimi, N., Galehdar, M. N., Moradi, and A. Moayyedkazemi, 2020. Green synthesis and characterization of copper nanoparticles and their effects on liver function and hematological parameters in mice. *Turkish Journal of Pharmaceutical Sciences*, 17(4), 412–416. <https://doi.org/10.4274/tjps.galenos.2019.28000>
14. Kiruba Daniel, S. C. G., G., Vinothini, N., Subramanian, K., Nehru, and M. Sivakumar, 2013. Biosynthesis of Cu, ZVI, and Ag nanoparticles using *Dodonaea viscosa* extract for antibacterial activity against human pathogens. *Journal of Nanoparticle Research*, 15(1). <https://doi.org/10.1007/s11051-012-1319-1>
15. Kulkarni, V. D., and P. S. Kulkarni, 2013. International Journal of Chemical Studies Green Synthesis of Copper Nanoparticles Using *Ocimum*. *International Journal of Chemical Studies*, 1(3), 1–4
16. Kuppusamy, P., M. M., Yusoff, G. P., Maniam, and N. Govindan, 2016. Biosynthesis of metallic nanoparticles using plant derivatives and their new avenues in pharmacological applications – An updated report. *Saudi Pharmaceutical Journal*, 24(4), 473–484. <https://doi.org/10.1016/j.jsps.2014.11.013>
17. Lee, H., Lee, G., N. R., Jang, J. H., Yun, J. Y., Song, and B. S. Kim, 2011. Biological synthesis of copper nanoparticles using plant extract Characterization of Copper Nanoparticles 2 . 3 Chemical Synthesis of Copper. *NSTI-Nanotech*, 1(1), 371–374
18. Magashi, A. M., and U. Abdulmalik, 2018. GC-MS and HPLC analysis of crude extracts

- of stem bark of *Adansonia digitata*. *Bayero Journal of Pure and Applied Sciences*, 10(1), 155. <https://doi.org/10.4314/bajopas.v10i1.32s19>.
19. Mehmood, S., N. K., Janjua, F., Saira, and H. Fenniri, 2016. AuCu@Pt nanoalloys for catalytic application in reduction of 4-nitrophenol. *Journal of Spectroscopy*, 2016. <https://doi.org/10.1155/2016/6210794>
20. Murthy, H. C. A., T., Desalegn, M., Kassa, B., Abebe, and T. Assefa, 2020. Synthesis of Green Copper Nanoparticles Using Medicinal Plant *Hagenia abyssinica* (Brace) JF. Gmel. Leaf Extract: Antimicrobial Properties. *Journal of Nanomaterials*, 2020. <https://doi.org/10.1155/2020/3924081>
21. Muthu, K., and S. Priya, 2017. Green synthesis, characterization and catalytic activity of silver nanoparticles using *Cassia auriculata* flower extract separated fraction. *Spectrochimica Acta - Part A: Molecular and Biomolecular Spectroscopy*, 179, 66–72. <https://doi.org/10.1016/j.saa.2017.02.024>
22. Pisoschi, A. M., and G. P. Negulescu, 2012. Methods for Total Antioxidant Activity Determination: A Review. *Biochemistry & Analytical Biochemistry*, 01(01), 1–10. <https://doi.org/10.4172/2161-1009.1000106>
23. Saranya, K., & Divyabharathi, U. (2019). Gas Chromatography and Mass Spectroscopic Analysis of Phyto- Compounds In *Dodonaea Viscosa* Leaf Extract. *Pramana Research Journal*, 9(9), 26–35
25. Saratale, R. G., H. S., Shin, G., Kumar, G., Benelli, D. S., Kim, and G. D. Saratale, 2018. Exploiting antidiabetic activity of silver nanoparticles synthesized using *punica granatum* leaves and anticancer potential against human liver cancer cells (HepG2). *Artificial Cells, Nanomedicine and Biotechnology*, 46(1), 211–222. <https://doi.org/10.1080/21691401.2017.1337031>
26. Shende, S., N., Gaikwad, and S. Bansod, 2016. Synthesis and evaluation of antimicrobial potential of copper nanoparticle against agriculturally important Phytopathogens. *International Journal of Biology Research*, 1(4), 41–47
27. Sierra-Ávila, R., M., Pérez-Alvarez, G., Cadenas-Pliego, V., Comparán Padilla, C., Ávila-Orta, O., Pérez Camacho, E., Jiménez-Regalado, E., Hernández-Hernández, and R. M. Jiménez-Barrera, 2015. Synthesis of Copper Nanoparticles Using Mixture of Allylamine and Polyallylamine. *Journal of Nanomaterials*, 2015. <https://doi.org/10.1155/2015/367341>
28. Thakur, S., S., Sharma, S., Thakur, and R. Rai, 2018. Green Synthesis of Copper Nanoparticles Using *Asparagus adscendens* Roxb. Root and Leaf Extract and Their Antimicrobial Activities. *International Journal of Current Microbiology and Applied Sciences*, 7(04), 683–694. <https://doi.org/10.20546/ijcmas.2018.704.077>
29. Tripathi, R. M., N., Kumar, A., Shrivastav, P., Singh, and B. R. Shrivastav, 2013. Catalytic activity of biogenic silver nanoparticles synthesized by *Ficus panda* leaf extract. *Journal of Molecular Catalysis B: Enzymatic*, 96(October 2017), 75–80. <https://doi.org/10.1016/j.molcatb.2013.06.018>
30. Younis, F. A. I., H., Abdelbagi, M., Ahmed, F., Ahmed, and R. Mohmmmed, 2018. Green Synthesis and Characterization of Gold Nanoparticles (AuNPs) Using Fenugreek Seeds Extract (*Trigonella foenum - gracum*). *European Journal of Biomedical and Pharmaceutical Sciences*, 5(4), 100–107
31. Zhang, K., J. M. Suh, , J. W., Choi, H. W., Jang, M., Shokouhimehr, and R. S. Varma, 2019. Recent Advances in the Nanocatalyst-Assisted NaBH₄ Reduction of Nitroaromatics in Water. *ACS Omega*, 4(1), 483–495. <https://doi.org/10.1021/acsomega.8b03051>